Donald G. Truhlar
Editor

Mathematical Frontiers in Computational Chemical Physics

With 89 Illustrations

Springer-Verlag
New York Berlin Heidelberg
London Paris Tokyo

COLLECTIVE PHENOMENA IN STATISTICAL MECHANICS AND THE GEOMETRY OF POTENTIAL ENERGY HYPERSURFACES

FRANK H. STILLINGER†

Abstract. Static and dynamic properties in dense many-body systems are considered from a unified point of view that emphasizes geometric features of the potential energy function Φ for interparticle interactions. Steepest descent mapping on the Φ hypersurface generates a natural division of the multidimensional configuration space into "basins" whose boundaries contain the fundamental transition states for the system as a whole. The resulting statistical representation (a) identifies an inherent structure for the liquid state, (b) leads to a simple description of phase transitions, (c) offers a natural formalism for supercooled liquids, and (d) provides an analysis of relaxation phenomena in glasses. Classical mechanics is used throughout the development.

1. Introduction. The condensed phases of matter (crystalline, liquid, amorphous solid, liquid-crystalline, quasicrystalline, etc.) display a fascinating variety of "collective" properties whose existence stems from the strong and often complicated intermolecular forces that are present. Predicting and understanding these collective phenomena from just a knowledge of intermolecular forces has been an enduring challenge to statistical mechanics. In spite of some remarkable successes, the subject remains open. The object of these three lectures is to develop a comprehensive framework for studying collective phenomena in condensed matter, to demonstrate some of the new insights it produces, and most importantly to identify some outstanding mathematical questions that it generates.

2. Condensed systems. By definition, the constituent particles (atoms, molecules) of a sample of dense matter are in continuing interaction with one another. The interactions are comprised in a potential energy function $\Phi(\mathbf{r}_1 \ldots \mathbf{r}_N)$, whose variables $\mathbf{r}_i$ represent the position coordinates of the N particles. Generally, Φ is bounded below by $-KN$ for some $K > 0$, is at least twice differentiable in all its variables when no pair of particles overlap, and vanishes when all particles recede infinitely far from one another.

A simple (but still challenging!) class of Φ's is frequently used in statistical mechanical modeling, namely a sum of particle pair interactions. When all N particles are identical, one then has

$$\phi(\mathbf{r}_1 \ldots \mathbf{r}_N) = \sum_{i<j=1}^{N} v(\mathbf{r}_i, \mathbf{r}_j). \tag{2.1}$$

If the particles furthermore are just atoms or ions, the pair potential v would depend only on distances r_ij.

The temporal evolution of the N-particle system is determined by its dynamical equations, and these depend on Φ. For simplicity it will be assumed that classical mechanics applies, *i.e.*, Newton's equations of motion are relevant.

†AT&T Bell Laboratories, Murray Hill, New Jersey 07974, USA

If the total system energy is large enough it is normally expected that the N-body system would be able to achieve thermal equilibrium at some absolute temperature T. If this is so, thermodynamic properties can be derived from the canonical partition function Z_N which in classical statistical mechanics has the following form [1]:

$$Z_N(\beta) = (\lambda_T^{3N} N!)^{-1} \int d\mathbf{r}_1 \cdots \int d\mathbf{r}_N \exp(-\beta\Phi), \tag{2.2}$$

where $\beta = (k_B T)^{-1}$, k_B is Boltzmann's constant, and λ_T is the mean thermal de Broglie wave length (independent of Φ, and irrelevant in most of the following). Integration limits on the $\mathbf{r}_i$ are determined by the containment vessel for the material sample which we assume has volume V. The logarithm of Z_N gives $-\beta$ times the Helmholtz free energy F for the system, from which standard thermodynamic formulas allow pressure, energy, entropy, $\cdots$, to be obtained. It is usually the case (as in this presentation) that primary interest concerns the large-N limit with temperature and density held constant.

No generating function analogous to Z_N is available to produce properties in the general nonequilibrium regime. Instead one may be obliged to consider the full details of Newtonian dynamical orbits to extract nonequilibrium behavior.

2.1 Steepest descent mapping. No general exact procedures are available to evaluate multiple integrals of the type in Z_N, Eq. (2.2), even for pairwise additive potentials. However, a series of transformations can be applied that creates formal simplifications and that has important conceptual advantages [2]. These transformations are generated by Φ itself.

For rotational simplicity let $\mathbf{R} \equiv (\mathbf{r}-1 \cdots \mathbf{r}_N)$, $\Phi \equiv \Phi(\mathbf{R})$, and suppose that we are dealing with structureless point particles in ordinary 3-space so that $\mathbf{R}$ has $3N$ components. Steepest-descent trajectories on the Φ hypersurface in $(3N+1)$-space are generated by solutions to

$$\partial\mathbf{R}/\partial\tau = -\nabla\Phi(\mathbf{R}), \tag{2.3}$$

where τ is a "virtual time" variable. These trajectories "relax" the collection of particles, moving each one at a velocity proportional to the force it experiences, until (as $\tau \to +\infty$) the steepest-descent trajectory lodges at a local minimum of Φ. Thus the solutions to Eq. (2.3) generate a mapping of (almost) all particle configurations $\mathbf{R}$ onto a discrete set of configurations $\mathbf{R}_\alpha$ which are the local minima of Φ. Here we use α as an index for local minima.

The connected set of particle configurations all of which map onto minimum α defines a "basin" B_α. The collection of such basins essentially covers the entire $3N$-dimensional configuration space available to the particles. Basin boundaries are exceptional since Eq. (2.3) does not unambiguously map them to minima, but they constitute a zero-measure set with no consequence in the following.

It has been argued on simple intuitive grounds [2] that if all N particles are identical and are confined to a container with volume proportional to N, then in

the large-N limit the number $\Omega_0(N)$ of Φ minima should behave as

$$\Omega_0(N) = N! \exp[\nu N + o(N)], \tag{2.4}$$

where ν is positive and depends on container volume V. The $N!$ factor simply acknowledges that permuting particle positions converts any munimum to an essentially equivalent one.

There is a substantial need to validate Eq. (2.4) on a mathematically sound basis. It would be useful if bounds on ν could be supplied that are sharp enough to show how this quantity depends on number density N/V and on details of Φ. Another mathematical challenge concerns whether basins B_α are always simply connected, or whether some physically sensible Φ's produce multiple connectivity.

2.2 Partition function transformations. Steepest-descent basins can usefully be classified according to ϕ, their depths on a per-particle basis:

$$\phi = \Phi(\mathbf{R}_\alpha)/N. \tag{2.5}$$

Since the number of minima is large, and since the Φ's should be bounded between finite limits, it should be possible to define a distribution G of minima versus ϕ. In the large-N limit this distribution must have a form consistent with Eq. (2.4), namely

$$G(\phi) \sim N! \exp[N\sigma(\phi)] \tag{2.6}$$

where $\sigma(\phi)$ is independent of N but generally will vary with particle density.

An intrabasin configurational integral I_α at inverse temperature β may be defined for B_α as follows:

$$I_\alpha(\beta) = \int_{B_\alpha} d\mathbf{R} \exp[-\beta \Delta_\alpha \Phi(\mathbf{R})], \tag{2.7}$$

$$\Delta_\alpha \Phi(\mathbf{R}) = \Phi(\mathbf{R}) - \Phi(\mathbf{R}_\alpha). \tag{2.8}$$

It includes, with appropriate Boltzmann-factor weighting, all possible "vibrational" excursions away from the basin bottom. Not all basins of a given depth have the same shapes or I_α's, but it makes sense to lump those in a narrow depth interval $\phi \pm \epsilon$ together and to use the resulting average I_α to define a "vibrational free energy per particle" $f_v(\beta, \phi)$:

$$f_v(\beta, \phi) = -\lim_{\epsilon \to 0} \lim_{N \to \infty} (N\beta)^{-1} \ln \langle I_\alpha(\beta) \rangle_{\phi \pm \epsilon}. \tag{2.9}$$

Armed with definitions (2.6) and (2.9) for σ and f_v, one finds that for large N the partition function Z_N has the following asymptotic representation:

$$Z_N(\beta) \sim \lambda_T^{-3N} \int d\phi \exp\{N[\sigma(\phi) - \beta\phi - \beta f_v(\beta, \phi)]\}. \tag{2.10}$$

The original multiple integral of high order, Eq.(2.2), has been replaced by a simple quadrature. In addition, the problem has been clearly separated into a purely enumerative part (σ), and a thermal vibration part (f_v).

Since N is large, the dominant contribution to the integral in Eq. (2.10) is provided by the maximum of the integrand, *i.e.* $-\beta$ times the Helmoholtz free energy per particle is given by

$$
\begin{aligned}
&-\beta F/N = (\ln Z_N)/N \\
&\cong -3\ln\lambda_T + \sigma(\phi_m) - \beta\phi_m - \beta f_v(\beta,\phi_m) \qquad (2.11)
\end{aligned}
$$

(with an error that vanishes in the large-N limit), where $\phi_m(\beta)$ is determined by the criterion:

$$
\sigma(\phi_m) - \beta\phi_m - \beta f_v(\beta,\phi_m) = maximum. \qquad (2.12)
$$

The significance of $\phi_m(\beta)$ is that it gives the depth of those basins that dominate equilibrium properties at the given temperature and density. It seems clear that ϕ_m must be a decreasing function of $\beta = 1/k_\beta T$, and as $\beta \to +\infty\phi_m$ approaches the potential energy per particle for the global ϕ minimum (normally expected to correspond to a crystalline arrangement of the N particles).

Although it may be difficult generally to determine the enumeration function σ for a given potential function Φ, the inverse problem might be amenable: Given $\sigma(\phi)$, is it possible to construct a potential which has this as its local minimum enumeration function?

Generalizations of the foregoing to include the case of several distinguishable species are conceptually trivial.

2.3 Particle pair distribution functions. The distribution of distances between particle centers has experimental significance, since it can be measured by X-ray or neutron diffraction. The theoretical significance is that when Φ is pairwise additive and the particles are spherically symmetric, the thermodynamic energy and pressure can be expressed as simple quadratures of the distance distribution.

Conventionally the distance distribution is presented as the pair correlation function $g^{(2)}(s)$. At equilibrium in a single-species system it is given by [1]:

$$
g^{(2)}(s) = \frac{\int d\mathbf{r}_1 \cdots \int d\mathbf{r}_N \delta(s - r_{12}) \exp(-\beta\Phi)}{B(s) \int d\mathbf{r}_1 \cdots \int d\mathbf{r}_N \exp(-\beta\Phi)}, \qquad (2.13)
$$

where

$$
r_{12} = |\mathbf{r}_2 - \mathbf{r}_1|, \qquad (2.14)
$$

$$
B(s) = B(s) = V^{-2} \int d\mathbf{r}_1 \int d\mathbf{r}_2 \delta(s - r_{12}), \qquad (2.15)
$$

and δ is the Dirac-delta function. When s is large compared to the range of intermolecular forces, $g^{(2)}$ is essentially independent of s. For small s it reflects the

way that interactions produce preferred spatial arrangements of particles. Generally, s variations of $g^{(2)}$ have greater amplitude at low temperature then at high temperature.

Steepest-descent mapping is applicable to the distribution of pair distances, and produces a remarkable "image enhancement" effect. The corresponding "quenched pair correlation function" $g_q^{(2)}(s)$ can be written in a form analogous to that of Eq. (2.13):

$$g_q^{(2)}(s) = \frac{\int d\mathbf{r}_1 \cdots \int d\mathbf{r}_N \delta[s - r_{12q}(\mathbf{r}_1 \cdots \mathbf{r}_N)] \exp(-\beta\Phi)}{B(s) \int d\mathbf{r}_1 \cdots \int d\mathbf{r}_N \exp(-\beta\Phi)}. \tag{2.16}$$

Here r_{12q} is the scalar distance between particles 1 and 2 *after* the steepest descent mapping has been applied to configuration $\mathbf{r}_1 \cdots \mathbf{r}_N$. Consistent with previous remarks, $g_q^{(2)}$ is the result of removing intra-basin vibrational deformations from $g^{(2)}$.

Molecular dynamics computer simulation results are now aviailable, giving both $g^{(2)}$ and $g_q^{(2)}$ for some simple atomic models [3]. Figure 1 schematically presents the principal result, namely that virtually all of the temperature dependence of the conventiaonal $g^{(2)}$ for liquids stems from intra-basin processes. More precisely, under constant density conditions, $g_q^{(2)}$ is essentially independent of the temperature of the starting liquid, provided that the temperature is at or above the thermodynamic melting temperature. Hence $g_q^{(2)}$ represents the inherent structure present in the liquid state. That such a temperature-independent inherent structure should exist seems (from computer simulation studies) to be connected with the narrowness of the distribution of basin depths, *i.e.*, the curvature of $\sigma(\phi)$ near its maximum. But why the vast majority of minima should be so closely spaced in ϕ is still an unanswered question.

In several popular many-body models, Φ has the additive form shown in Eq. (2.1) with a central pair potential that diverges at the origin thus:

$$v(r) \sim Ar^{-p} \quad (r \to 0), \tag{2.17}$$

where $A > 0$, $p > 3$. Under equilibrium conditions it is widely believed that the corresponding small-r behavior of the pair correlation function will be ($\beta = 1/k_B T$):

$$\ln g^{(2)}(s) \sim -\beta A s^{-p} \quad (s \to 0). \tag{2.18}$$

The steepest-descent mapping is expected to produce a function $g_q^{(2)}$ which, like $g^{(2)}(s)$, vanishes strongly at the origin. But does $\ln g_q^{(2)}$ behave as $-(const)s^{-p}$, or is a fundamentally different asymptote involved? Once again no answers yet exist.

3. Phase transitions. Phase transitions are dramatic examples of the collective phenomena exhibited by condensed matter. They include melting and freezing, spontaneous changes of crystal symmetry, transitions that form or destroy liquid crystals, and a variety of surface reconstructions on both crystalline and liquid substrates. Understanding and controlling phase transitions is scientifically compelling and technologically urgent.

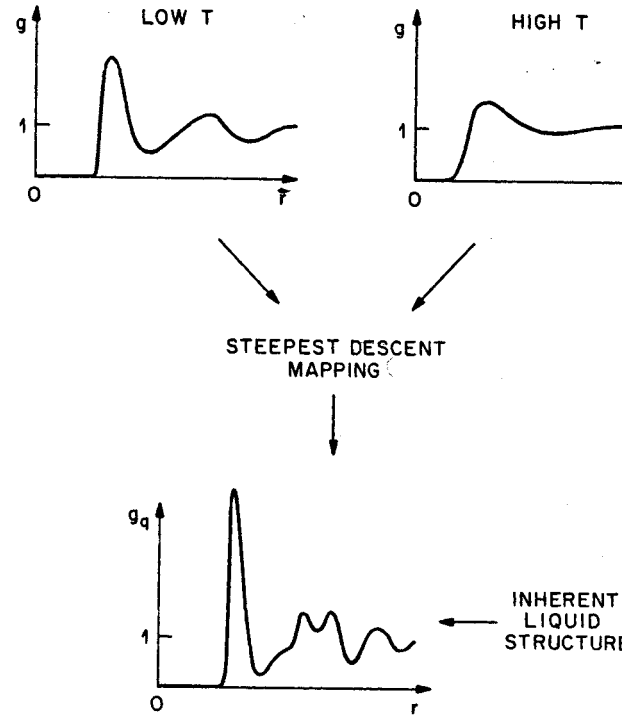

Figure 1. Inherent structure in the liquid state revealed by steepest descent quenching.

The formalism presented in Sect. 2 offers a convenient way to discuss and to analyze phase transitions of the types just mentioned. Since it is fundamentally a classical statistical-mechanical approach, it cannot in its present form describe those transitions (metal-insulator, normal metal-superconductor, helium Bose condensation, ...) whose basis is explicitly quantum mechanical.

For the most part this Section will be concerned with thermodynamic equilibrium aspects of phase change (Sects. 3.1–3.3). However, in Sect. 3.4 Section E we will briefly consider the properties of long-lived metastable states, such as supercooled liquids.

3.1 Order-disorder transition in substitutional alloys. Solid state physics offers several examples of crystalline binary alloys whose component atoms A and B have an alternating periodic arrangement at low temperature, but are disordered among the crystal sites at high temperature (but still below the alloy's melting point). A thermodynamic phase transition separates these two regimes. A well-known case is β-brass, incorporating equal numbers of copper and zinc atoms in a body-centered cubic structure (see Figure 2). Copper atoms are segregated on one

of the simple cubic sublattices at low temperature, zinc atoms on the other. At high temperature the sublattices have equal occupancies due to thermally driven random substitutions. A phase transition between ordered and disordered forms occurs at about $460°C$, accompanied by an infinite heat capacity anomaly [4].

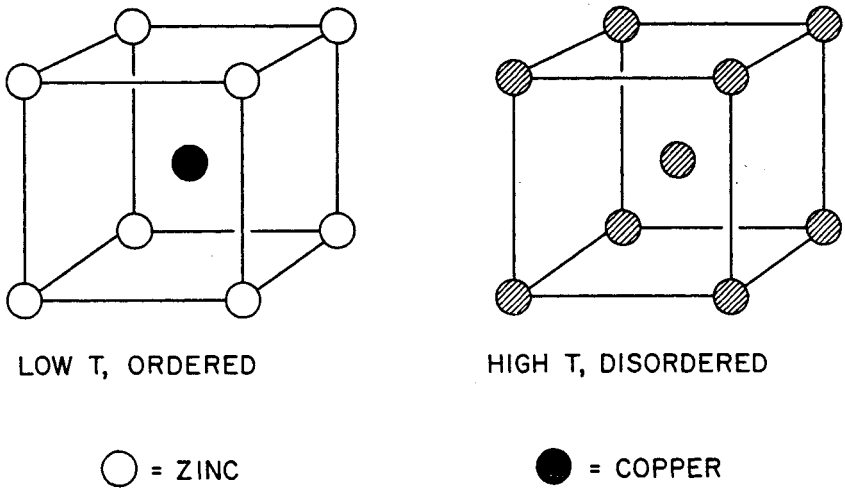

Figure 2. Atomic arrangements in the ordered low temperature and disordered high temperature forms of β-brass.

β-brass melts of course (at about $850°C$), and the system then moves in regions of its configuration space whose basins β_α have minima corresponding to amorphous atom packings. However, these regions of configuration space are not at issue in discussing the order-disorder transition. For simplicity we can restrict attention just to those basins and their minima corresponding to equal numbers (say $N/2$) of copper (A) and zinc (B) atoms arranged on the sites of a perfect body-centered cubic lattice. The distribution of potential energy minima for this two-species system restricted to the crystalline state may be written asymptotically as follows:

$$G(\phi) = [(N/2)!]^2 \exp[N\sigma(\phi)] \tag{3.1}$$

where as before ϕ is the potential energy per atom at the minima of the total potential energy function Φ.

The physics of these substitutional alloys suggests two convenient simplifying assumptions. The first is that the Φ_α, the local minima of Φ, depend only on the interactions of nearest-neighbor atom pairs. This is equivalent to the statement

$$\Phi_\alpha = Na + N_\ell b, \tag{3.2}$$

where a and b are constants and N_ℓ is the number of nearest-neighbor like-atom pairs. We must have

$$b > 0 \tag{3.3}$$

so that the absolute Φ minimum has $N\ell = 0$ (A and B segregated on separate sublattices with each A having eight B's as nearest neighbors, and vice versa).

The second simplifying assumption is that the vibrational properties, specifically $f_v(\beta, \phi)$, are the same regardless of the atomic arrangement over the body-centered cubic lattice. Under this circumstance the dominant basin depth at any given inverse temperature β which we have denoted by $\phi_m(\beta)$, can be obtained from a simplified form of Eq. (2.12),

$$\sigma(\phi_m) - \beta\phi_m = maximum \tag{3.4}$$

or equivalently (since σ'' seems always to be nonpositive),

$$\sigma'(\phi_m) = \beta. \tag{3.5}$$

Equation (3.2) states that ϕ is a linear function of N_ℓ/N, and it is clear that

$$a \leq \phi \leq a + 4b. \tag{3.6}$$

In the randomly substituted state ϕ is just at the middle of this range, $a + 2b$.

Evaluation of $\sigma(\phi)$ is an enumeration problem, namely "How many ways can $N/2$ A's plus $N/2$ B's be placed on a body-centered-cubic lattice so that there are exactly $N_\ell(\equiv N_\phi/b)$ nearest-neighbors atom pairs of like species?" Exactly the same enumeration problem lies at the heart of the Ising model on the same lattice (atoms A and B are equivalent to up and down spins in the Ising model)[1]. Although two-dimensional Ising models have been solved exactly [5], only approximate results are avilable for three-dimensional cases. Nevertheless a variety of techniques have been applied (series analysis, renormalization group methods, Monte Carlo computer simulations) that seem to reveal the principal features of interest.

A graphical construction for $\phi_m(\beta)$ corresponding to the determing in Eq. (3.5) involves rolling a straight line (slope β) on the curve of σ versus ϕ. The order-disorder transition point ($\beta = \beta_c$) is associated with a vanishing-curvature singularity of $\sigma(\phi)$ in the neighborhood of which we have

$$\sigma(\phi) = \sigma(\phi_c) + \beta_c(\phi - \phi_c) - A_\pm|\phi - \phi_c|^{p_\pm} + \ldots, \tag{3.7}$$
$$A_\pm > 0, \quad p_\pm > 2, \quad \phi_c = \phi_m(\beta_c),$$

where subscripts $+$ and $-$ refer respectively to $\phi > \phi_c$ and $\phi < \phi_c$. Terms beyond those shown in Eq. (3.7) have higher powers of $|\phi - \phi_c|$ than $p_\pm$.

By carrying out the construciton of $\phi_m(\beta)$ near β_c graphically or otherwise, we find

$$\phi_m(\beta) - \phi_c = \left(\frac{\beta_c - \beta}{p_+ A_+}\right)^{1-\alpha_+} + \ldots, \quad (\beta < \beta_c), \tag{3.8a}$$

$$\phi_c - \phi_m(\beta) = \left(\frac{\beta - \beta_c}{p_- A_-}\right)^{1-\alpha_+} + \ldots, \quad (\beta > \beta_c), \tag{3.8b}$$

where

$$\alpha_{\pm} = \frac{p_{\pm} - 2}{p_{\pm} - 1} > 0. \tag{3.9}$$

A β derivative of these potential energy expressions produces essentially the heat capacity $C_{\pm}$, which we therefore see exhibits the characteristic divergence exponent(s) $\alpha_{\pm}$.

$$C_{\pm}(\beta) = K_{\pm}|\beta - \beta_c|^{-\alpha_{\pm}} + \ldots. \tag{3.10}$$

Experimental measurements, and the various approximate theories of order-disorder critical phenomena for 3-dimensional systems seem to agree that critical exponent $\alpha_{\pm}$ is small and of the order of 0.1. But it remains a challenge to combinatorial mathematics to provide an exact evaluation of heat capacity and other critical exponents, perhaps by obtaining the relevant $\sigma(\phi)$.

3.2 Melting and freezing transitions. The order-disorder phase transition just described is a "continuous" phase transition. Any property evaluated in the low-temperature ordered phase and in the high-temperature disordered phase respectively approaches the same limit as T approaches $T_c = (k_B\beta_c)^{-1}$ from either side. This contrasts vividly with "discontinuous" or "first-order" phase transitions where the two phases involved remain distinctly different at any temperature where both can exist. We will now consider the case of melting in single-component substances, where the low-temperature crystal transforms discontinuously to the liquid; the two phases differ in symmetry, mechanical properties, density, and energy.

The convention we have used is that the container volume V is kept fixed as temperature changes, and as steepest-descent mappings are effected. Under circumstances the singularity structure of $\sigma(\phi)$ will be influenced by the *constant-pressure* densities of the crystal and liquid. If these differ (as is virtually always the case) then at *constant volume* the crystal melting temperature T_m will be less than the liquid freezing temperature T_f. In the intervening interval

$$T_m < T < T_f, \tag{3.11}$$

the system displays coexisting macroscopic regions of crystal and liquid, *i.e.*, a mixed state with proportions of crystal and liquid varying continuously with T.

Although it was reasonable to suppose that the basin vibrational free energy $f_v(\beta, \phi)$ was independent of ϕ in the preceding order-disorder example, that is no longer the case for the melting-freezing transition. The crystal and liquid phases are structurally too unlike to permit such an approximation. Just as does $\sigma(\phi)$, $f_v(\beta, \phi)$ is now expected to exhibit nontrivial ϕ variation and to show a singularity structure consistent with phase coexistence.

Figure 3 indicates the graphical relationsip of the terms in Eq. (2.12) at the endpoints of the coexistence interval (3.11). Matching of slopes for σ and for $\beta(\phi + f_v)$ as before locates $\phi_m(\beta)$. When coexistence obtains, the steepest descent mapping of

particle configurations presumably produces mechanically stable particle packings which themselves exhibit coexistence. That is, the dominant packings identified by $\phi_m(\beta)$ in this temperature interval will have large side-by-side regions respectively with ordered and with disordered particle arrangements. To show that such heterogeneous packings exist for physically reasonable potentials is a nontrivial matter, but accumulating computer simulation data demonstrates that it is so [6].

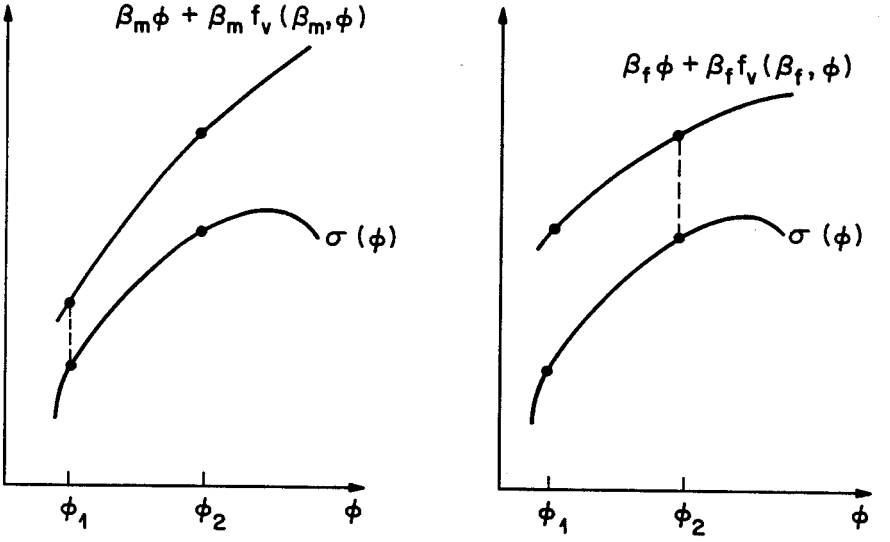

Figure 3. Matching of slopes for terms in Eq. (I.11) for the crystal-liquid first-order phase transition. The left panel corresponds to the fixed-volume melting point of the crystal, the right panel to the freezing point of the liquid.

The most basic unanswered questions concerning this description involve the nature of the singularities, with respect to ϕ, of $\sigma(\phi)$ and of $f_v(\beta,\phi)$ at coexistence endpoints ϕ_1 and ϕ_2. These singularities are unlike that in the order-disorder case since the heat capacity remains finite at constant volume. The best present guess is that essential singularities are involved, and that these arise from "heterophase fluctuations," a distribution of small inclusions of one type of packing within large domains of the other type [7].

3.3 Two examples. We now focus attention on two models that have been extensively studied with computer simulation (molecular dynamics and Monte Carlo), and which exhibit melting and freezing phenomena. They both entail pairwise additive potential energy functions as in Eq (2.1), with structureless point particles. Disregarding trivial constants the respective pair potentials are the inverse power potential.

(3.12) $$v(r) = r^{-p} \quad (p > 3)$$

and the Gaussian core potential

$$v(r) = \exp(-r^2). \tag{3.13}$$

Both involve only repulsive forces. The restriction on p in the first of these is necessary to keep energy, entropy, and free energy extensive (*i.e.*, proportional to N).

The inverse power potential is a homogeneous function of distance, the implications of which are significant in the present connection. In particular it means that the density (ρ) and inverse-temperature (β) variations of σ and f_v must have the forms:

$$\sigma(\phi, \rho) \equiv \overline{\sigma}(\rho^{-p/3}\phi) \tag{3.14}$$

and

$$\beta f_v(\beta, \phi, \rho) \equiv y\overline{f}(\rho^{-p/3}\phi, y), \tag{3.15}$$

where

$$y = \beta\rho^{p/3}. \tag{3.16}$$

These follow from the fact that dilation and compression neither create nor destroy relative minima, but simply rescale the coordiunates that yield those minima. The structure of the low-temperature crystal is face-centered-cubic; relations (3.14) and (3.15) imply that the melting and freezing points correspond to fixed values of the parameter y.

The analytical properties of the Gaussian core potential are quite different. First, there is a duality relation between the low-density and high-density absolute minima of ϕ [8]:

$$\rho_f^{-1/2}[1 + 2\phi_f(\rho_f)] = \rho_b^{-1/2}[1 + 2\phi_b(\rho_b)], \tag{3.17a}$$

$$\rho_f\rho_b = \pi^{-3}. \tag{3.17b}$$

Here the subscripts f and b refer to the respective stable crystal forms, face-centered cubic at low density, body-centered cubic at high density. This identity stems from the self-similarity of the Gaussian function under Fourier transformation. The density at which the two crystal forms have equal energy is obvious from (3.17), namely

$$\rho = \pi^{-3/2}. \tag{3.18}$$

A second analytical property of the Gaussian core potential is that in the high density limit the energies of all periodic structures (even with very large unit cells) become asymptotically equal. More precisely the energy differences between distinct periodic structures go to zero (apparently) as $\exp(-C\rho^{2/3})$, $C > 0$. This implies that the melting and freezing temperatures vanish in the limit $\rho \to +\infty$. However, it is by no means clear at present how the basic quantities σ and f_v individually behave in this limit. Input from interested mathematicians on this question would certainly be welcome and illuminating.

3.4 Supercooling. Although the basic criterion (1.12) was formulated to describe strict equilibrium conditions, it is nevertheless also suggestive concerning a specific deviation from equilibrium, namely the supercooling of liquids below their freezing point. Careful experiments show that this is a repeatable and reproducible phenomenon, and a little thought suggests how Eq. (1.12) should be modified to describe that situation.

It seems clear that only a subset of potential minima and their basins should be considered. Supercooled liquids have avoided nucleation. The relevant packings therefore must be devoid of crystal fragments, at least those beyond some critical size. In principle this requires implementing an algorithm to decide if any packing is devoid of such crystallinity. It would clearly be useful to exhibit such an algorithm explicity and to determine if its implementation is a polynomial-time or an NP-complete problem [9].

The "amorphous" subset of packings which meet the noncrystallinity criterion can be enumerated just as before by a function $\sigma_a(\phi)$, where

$$\sigma_a(\phi) \leq \sigma(\phi). \tag{3.19}$$

This amorphous packing subset then will have a well-defined vibrational free energy function $f_{va}(\beta, \phi)$ in analogy to Eq. (1.9). Finally, then, the "quasi-equilibrium" condition for supercooled liquids has a form directly analogous to Eq. (1.12):

$$\sigma_a(\phi_{ma}) - \beta\phi_{ma} - \beta f_{va}(\beta, \phi_{ma}) = \text{maximum}. \tag{3.20}$$

The optimizing $\phi_m a(\beta)$ locates the depth of the dominating potential minima within the noncrystalline subset.

By projecting out of consideration the crystal-containing packings, the singularities present originally in σ and f_v which were associated with melting and freezing necessarily have been eliminated. It will be important to establish eventually whether σ_a and $f_v a$ display new singularities as might be associated, for instance, with a low-temperature glass transition or an instability point for strongly supercooled liquids. In any case it would be important to determine the lowest potential energy in the amorphous subset, what geometrical packing structure is involved, and how these attributes depend on the details of the algorithm employed to identify that subset.

Finally we note that pair correlation functions (both pre-quench and post-quench) can be precisely defined on the amorphous subset. Once again it would be important to determine how algorithm-sensitive are these functions.

4. Rate processes. Many-body systems in a condensed state display a wide variety of time-dependent collective properties. These include self diffusion, viscous flow, fracture, shock-wave propagation, crystal nucleation, and in some cases chemical reactions. Observable time dependence arises from the motion of the system configuration point $R(t)$ which in classical dynamics obeys the multi-dimensional Newton equation (masses taken to be unity):

$$d^2\mathbf{R}(t)/dt^2 = -\nabla\Phi[\mathbf{R}(t)]. \tag{4.1}$$

In virtually all cases of interest the dynamics occurs at sufficiently large (conserved total energy that the system is not trapped in any single basin B_α, but is more or less free to roam through a sequence of basins.

4.1 Collective transition states. With respect to the potential energy hypersurface, the least costly dynamical pathway between two contiguous basins passes through a "transition state" located on the common boundary hypersurface between the basins. This transition state is a horizontal saddle point with a single negative principal curvature, *i.e.*, it is characterized by a vanishing of $\nabla\Phi$ and by the existence of a single negative eigenvalue of the Hessian matrix $\nabla\nabla\Phi$. The eigenvector corresponding to the negative eigenvalue is conventionally identified with the direction of the so-called "reaction coordinate" through the transition state.

One should keep in mind that two or more transition states could occur on the boundary between two contiguous basins. Furthermore, horizontal saddle points that are *not* transition states could occur in the interior of basins. The frequency of such occurrences and how they depend upon interparticle interactions is unknown at present.

The number of transition states, their distribution by height with respect to basin bottoms, their spectrum of curvatures, and other basic geometric characteristics are directly relevant to the understanding of rate processes and how fast they proceed at different temperatures.

Unfortunately no general procedure for locating saddle points in multidimensional surfaces is presently available, analogous to the steepest-descent method [Eq. (1.3)] for local minima. But the importance of transition states has often forced researchers to devise and employ inefficient search routines. One that has been used is the following [10]:

(1) Using molecular dynamics computer simulation with frequent steepest-descent mapping, locate two potential minima at $\mathbf{R}_1$ and $\mathbf{R}_2$ with contiguous basins.

(2) Construct the linear path between $\mathbf{R}_1$ and $\mathbf{R}_2$:

$$\mathbf{R}(\ell) = \ell\mathbf{R}_1 + (1-\ell)\mathbf{R}_2. \tag{4.2}$$

The potential energy $\Phi[\mathbf{R}(\ell)]$ along this path has relative minima at $\ell = 0$ and 1, and must have at least one relative maximum in between. Let $\mathbf{R}_3$ be the position along this connecting line which produces the largest relative Φ maximum. This is a first crude estimate of the transition state position.

(3) Consider the scalar function

$$\Psi(\mathbf{R}) = [\nabla\Phi(\mathbf{R})]^2; \tag{4.3}$$

its zeros are all minima and include all of the extrema of the original function Φ. Starting at $\mathbf{R}_3$, construct a steepest-descent path on the Ψ hypersurface to identify one of its minima at location $\mathbf{R}_4$.

(4) Check to see if the Hessian matrix for Φ has only one negative eigenvalue at $\mathbf{R}_4$. If it does, use the corresponding eigenvector as the direction for

infinitesimal displacements both positive and negative away from the saddle point, followed by Φ-hypersurface steepest descent to verify that the originally-selected minima are the ones for which this saddle point serves as transition state.

Clearly this is an unwieldy process. Improved procedures would be an important advance.

4.2 Localization. The steepest descent mapping of the continuous dynamical trajectory $\mathbf{R}(t)$ for the many-body system produces $\mathbf{R}_q(t)$, a piecewise constant function whose values are positions of the bottoms of basins successively visited by the system. The left and right side limits for $\mathbf{R}_q$ at each time t_i that a discontinuity is encountered are (with unit probability) the bottoms of contiguous basins. It is important to note that the corresponding configurational shifts between those minima:

$$\Delta\mathbf{R}_q(i) = \lim_{\epsilon\to 0}[\mathbf{R}_q(t_i+\epsilon) - \mathbf{R}_q(t_i-\epsilon)] \tag{4.4}$$

appear from computer simulation studies to exhibit a localization property [10]. Specifically this means that most of the change typically is concentrated on a small subset [$O(1)$] of the N particles, and furthermore the typical displacements of particles in the small subset are comparable to particle diameters. Correspondingly the potential energy changes only by $O(1)$ between these minima, in spite of the fact that it is an $O(N)$ quantity.

This localization property implies that the directions of the $\Delta\mathbf{R}_q(i)$ are far from uniformly distributed over the surface of the $(3N-1)$-sphere. Instead they are concentrated strongly so that all but a small number of direction cosines are essentially zero.

Computer simulation studies reveal another nontrivial feature. Only rarely do the individual (localized) transitions carry the N-body system through a particle permutation. This *could* conceivable take place as a pair of nearest neighbors rotates 180° about their centroid, or more generally as a close loop of particles executes simultaneous jumps around that loop. But such shifts are exeptional.

These observations about localization and rarity of direct permutational transsitions are based only on studies of N-body systems with short-range interactions. The conclusions might well be different for long-range interactions, particularly if oscillatory pair potentials were present. This aspect clearly needs further study.

4.3 Self diffusion. The self-diffusion constant D measures the rate at which Brownian motion moves particles about. In terms of the time-dependent displacement $\Delta\mathbf{r}_i(t)$ for particle i, for large t,

$$D \sim \langle|\Delta\mathbf{r}_i(t)|^2\rangle/6t. \tag{4.5}$$

Here it is assumed that the system is in thermal equilibrium. The diffusion process is simultaneously underway for all N particles, and it reflects the sequence of basins

visited in the $3N$-dimensional configuration space. On account of the localization property for elementary transitions, the number of exit channels from any basin to neighboring basins is $O(N)$, so that rate of transition is also expected to be $O(N)$. In other words the mean residence time in any basin is $O(N^{-1})$.

Evidence thus far available from simulations indicates that under steepest descent quenching, individual particles tend only to move by an amount comparable to their diameter. If that is generally the case an alternative expression for D can be written as follows:

$$D \sim \langle |\Delta \mathbf{r}_{iq}(t)|^2 \rangle / 6t. \tag{4.6}$$

The quantity $\Delta \mathbf{r}_{iq}(t)$ is the displacement of particle i from the basin bottom relevant at time 0 to that relevant at time t. It would be desirable to know if there is any difference in the way that expressions (4.5) and (4.6) approach D with increasing t, specifically which converges more rapidly.

Experimental and simulational data for D as a function of absolute temperature T are is often fitted to expressions of the form:

$$D(T) \cong D_0 T^{1/2} \exp[-E(T)/k_B T]. \tag{4.7}$$

where D_0 is a positive constant. The factor $T^{1/2}$ represents mean particle speed, and the exponential Boltzmann factor with positive $E(T)$ supposedly represents the probability of climbing up potential energy barriers. Indeed for many liquids in their thermodynamic stability range, E is approximately independent of temperature. However, it is not at all clear how $E(T)$ in Eq. (4.7) relates specifically to the distribution of transition state barrier heights between basins in the $3N$-dimensional configuration space. This remains an important research topic.

4.4 Glass transitions. We have already seen how a quasi-equilibrium description of supercooled liquids can be based on a subset of the configuration space basins. Its applicability requires that the system of interest (a) be able to explore the allowed basins adequately to achieve a representative sampling, while (b) avoiding nucleation (*i.e.*, penetration of the excluded set of crystalline basins). As a liquid is superecooled more and more its rate of basin exploration declines strongly, so that even if nucleation were to be avoided the quasi-equilibrium expression (3.20) must eventually become inapplicable to real experiments. For many substances this happens over a narrow temperature interval, often identified as a glass transition temperature T_g. Keep in mind that this is a somewhat ill-defined quantity, not on the same par as the precisely defined thermodynamic melting and freezing temperature.

Cooling well below T_g produces an amorphous solid whose properties depend upon the rate of cooling through T_g. In this low-temperature regime the system typically behaves as though it were trapped in a relatively small group of basins. The conserved total energy is so low that it is very unlikely or even impossible to find sufficiently low transition states as escape routes to surrounding basins. The self-diffusion constant becomes immeasurably small, consistent with the trapping.

As a supercooled liquid enters the glass transition regime, its time-dependent behavior (fluctuation, regression, and response to external perturbations) demonstrates the presence of a broad spectrum of relaxation times. Near T_g, various measurable properties vs. time often can be fitted to a "stretched exponential" decay

$$\exp[-(t/\tau)^{\beta_0}]; \quad 0.3 < \beta_0 < 1.0, \tag{4.8}$$

where β_0 can depend on temperature and τ increases rapidly as T decreases through the T_g range. Laplace-transforming (4.8) identifies a wide range of superposed simple exponential decay rates whose presence indicates the complexity of the potential energy hypersurface over which the system is sluggishly diffusing.

Clearly what is required is an appropriate description for the multiple-length-scale topography of the $3N$-dimensional Φ hypersurface in the amorphous region, and how that determines the wide spectrum of relaxation times. One approach, which exhibits some features of a "renormalization group" program, involves combining basins into metabasins [11]. Specifically, let basins B_α and B_β belong to the same metabasin $\overline{B}_\gamma$ if (a) B_α and B_β are inequivalent (not related simply by particle permutation), (b) B_α and B_β are either contiguous or are connected by a sequence of contiguous basins in the same metabasin, and (c) the barrier heights of the lowest transition states between B_α and B_β (either in a shared boundary, or along a chain of basins in the metabasin that connects them) do not exceed $\eta > 0$. Here we take η to measure the lesser elevation of the transition state measured from the two flanking minima.

As η increases, the original basins aggregate into a declining number of ever-larger metabasins. In analogy with Eq. (1.4), the η-dependent number of metabasins asymptotically can be written

$$\Omega(N, \eta) \sim N! \exp[\nu(\eta)N], \tag{4.9}$$

where ν is a strictly decreasing function of η.

Consider just the transitions between metabasins. These should include the longest relaxation times present in the system (they are evidently associated with large-scale topographic features of the Φ-scape), but should exclude rapid relaxation times. The dividing line roughly should occur for times proportional to the Boltzmann factor:

$$\exp(-\eta/k_B T). \tag{4.10}$$

The function $\nu(\eta)$ is a fundamental measure of the multidimensional Φ topography. Unfortunately it is poorly known, but obviously it must vanish as $\eta \to +\infty$. Heuristic arguments suggest that in order to produce relaxation spectra of the type underlying the stretched exponential function, $\nu(\eta)$ would have to possess roughly the following form:

$$\nu(\eta) \sim \exp[-A \exp(a\eta)], \quad A, a > 0 \tag{4.11}$$

wherein a is related to β_0 as follows:

$$\beta_0 = k_B T a/(1 + k_B T a), \qquad (T \approx T_g). \tag{4.12}$$

Quite obviously this loose heuristic connection between topography and relaxation rates needs substantial strengthening with rigorous analysis.

4.5 Dynamical recurrences. As a final matter, we consider briefly the return of the configuration-space dynamical trajectory $\mathbf{R}(t)$ to the basin B_α in which it was located at $t = 0$. This forms a kind of momentum-blind and spatially course-grained version of the venerable Poincaré recurrence problem in dynamics [12].

Let $U_\alpha(\mathbf{R})$ be the characteristic function for B_α, 1 inside and 0 outside. Consider the autocorrelation function

$$u(t) = \langle U_\alpha[\mathbf{R}(0)] U_\alpha[\mathbf{R}(t)] \rangle, \tag{4.13}$$

where the average involved is canonical *i.e.*, fixed temperature, and it includes all basins. Obviously $u(0) = 1$. The initial decay of $u(t)$ is related to the mean escape rate from basins. If the system is ergodic, the long-time limit should be determined essentially by the number of basins with depths given by ϕ_m, Eq. (1.12); that is:

$$\lim_{t \to \infty} u(t) = (N!)^{-1} \exp \{ - N \sigma[\phi_m(\beta)] \}. \tag{4.14}$$

Here it is assumed that most of the relevant basins for the given temperature are "typical."

The detailed behavior of $u(t)$ should reveal the statistics of return times. Those statistics should be particularly illuminating as temperature declines, raising the possibility of transition from ergodic to nonergodic regimes. Perhaps this could be related to the glass transition in a useful way.

REFERENCES

[1] T. L. Hill, *Statistical Mechanics*, McGraw-Hill, New York, 1956.

[2] F. H. Stillinger and T. A. Weber, *Hidden structure in liquids*, Phys. Rev. A, 25 (1982), pp. 978–988.

[3] F. H. Stillinger and T. A. Weber, *Inherent pair correlation in simple liquids*, J. Chem. Phys., 80 (1984), pp. 4434–4437.

[4] C. Kittel, *Introduction to Solid State Physics*, 2nd edition, Wiley, New York, 1956, p. 340.

[5] R. J. Baxter, *Exactly Solved Models in Statistical Mechanics*, Academic Press, New York, 1982.

[6] F. H. Stillinger and R. A. LaViolette, *Local order in quenched states of simple atomic substances*, Phys. Rev. B, 34 (1986), pp. 5136–5144.

[7] A. F. Andreev, *Singularity of thermodynamic quantities at a first order phase transition point*, Sov. Phys., JETP (English trans.), 18 (1984), pp. 1415–1416.

[8] F. H. Stillinger, *Duality relations for the Gaussian core model*, Phys. Rev. B, 20 (1979), pp. 299–302.

[9] M. R. Garey and D. S. Johnson, *Computers and Intractability: A Guide to the Theory of NP-Completeness*, W. H. Freeman, San Francisco, 1979.

[10] T. A. Weber and F. H. Stillinger, *Interactions, local order, and atomic rearrangement kinetics in amorphous nickel-phosphorous alloys*, Phys. Rev. B, 32 (1985), pp. 5402–5411.

[11] F. H. Stillinger, *Role of potential energy scaling in the low-temperature relaxation behavior of amorphous materials*, Phys. Rev. B, 32 (1985), pp. 3134–3141.

[12] A. Münster, *Prinzipien der statistischen Mechanik*, in *Handbuch der Physik, Band III/2, Prinzipien der thermodynamik und statistik*, ed. S. Flügge, Springer-Verlag, Berlin, 1959, pp. 216–218.